SPARSE BUMP MODELING OF MILDAD PATIENTS
Modeling Transient Oscillations in the EEG of Patients with Mild Alzheimer's Disease

François-Benoit Vialatte[a,1], Charles François Vincent Latchoumane[b], Nigel Hudson[c]
Sunil Wimalaratna[d], Jordi Solé-Casals[e], Jaeseung Jeong[b] and Andrzej Cichocki[a]
[a]*Riken BSI, Lab. ABSP, Wako-Shi, Japan*
[b]*KAIST, Dept of Bio and Brain Engineering, Daejeon, South Korea*
[c]*Derriford Hospital, Dept of Neurophysiology, Plymouth U.K.*
[d]*Radcliffe Infirmary, Dept of Neurology, Oxford, U.K.*
[e]*Digital Technologies Group,University of Vic, Vic, Spain*

Keywords: EEG, Alzheimer, Time-frequency, Bump, Local synchrony.

Abstract: We explore the potential of bump modeling to extract transient local synchrony in EEG, as a marker for mildAD (mild Alzheimer's disease). EEG signals of patients with mildAD are transformed to a wavelet time-frequency representation, and afterwards a sparsification process (bump modeling) extracts time-frequency oscillatory bursts. We observed that organized oscillatory events contain stronger discriminative signatures than averaged spectral EEG statistics for patients in a probable early stage of Alzheimer's disease. Specifically, bump modeling enhanced the difference between mildAD patients and age-matched control subjects in the θ and β frequency ranges. This effect is consistent with previous results obtained on other databases.

1 INTRODUCTION

Alzheimer's disease is a brain disorder, whose prevalence is dramatically increasing (due to the general increase of life expectancy), threatening our societies. It would be a great asset if we were able to detect it as early as possible. A cost-efficient technique would be necessary to screen populations at risk, potentially thousands to even millions of people. Electroencephalography (EEG) is cost-effective, and was suggested as a tool for diagnosing AD (Jeong, 2004); however its specificity to the disease is low, so that its reliability is sometimes questioned. Nevertheless, EEG data are not totally exploited by medical teams, especially its main advantage: a very precise time resolution, allowing investigations of brain dynamics (see (Jeong, 2004) for a review). Our purpose here is to explore the potential of transient local synchrony in EEG, as a marker for the early stages of Alzheimer's disease.

Brain signals evolve quickly and non-linearly in time. EEG recordings consist of stable and sustained activities on one hand, and unstable and transitory activities on the other hand. When these transitory activities become organized in patterns, they form bursts in EEG signals. Here, we are interested in these bursts, usually characterized as a succession of 4-5 oscillations, within a limited frequency range: they are hypothesized to be representative of transient synchronies of neural populations (Vialatte et al., 2007; Vialatte et al., 2009b; Vialatte et al., 2009c). In the past few years, a lot of attention was devoted to EEG signals evoked or induced by specific stimulations (see *e.g.* (Başar, 1980; Quiroga et al., 2001; Moratti et al., 2007; Nikulin et al., 2007; Klimesch et al., 2007; Vialatte et al., 2009b)). The brain responses to stimuli can be observed in EEG signals, and such oscillatory bursts can be part of this response. But this kind of activity is not shut down during rest periods. We intend here to study oscillatory bursts in EEG signals recorded in rest condition, at the single trial level (not using averaging, which is meaningless in this context). For this purpose, we applied bump modeling as a transient local synchrony marker for

[1]FBV was at KAIST, Dept of Bio and Brain Engineering, when this investigation was done

Vialatte F., François Vincent Latchoumane C., Hudson N., Wimalaratna S., Solé-Casals J., Jeong J. and Cichocki A. (2010).
SPARSE BUMP MODELING OF MILDAD PATIENTS - Modeling Transient Oscillations in the EEG of Patients with Mild Alzheimer's Disease.
In *Proceedings of the Third International Conference on Bio-inspired Systems and Signal Processing*, pages 479-484
DOI: 10.5220/0002755104790484

AD detection.

2 METHODS

2.1 EEG Data - Patients With MildAD

These data were obtained using a strict protocol from Derriford Hospital, Plymouth, U.K. and had been collected using normal hospital practices (Henderson et al., 2006). EEGs were recorded during a resting period with various states: awake, drowsy, alert and resting states with eyes closed and open. All recording sessions and experiments proceeded after obtaining the informed consent of the subjects or the caregivers and were approved by local institutional ethics committees. We used two EEG databases: database A and database B.

Database A was composed of 24 healthy control subjects (age: 69.4±11.5; 10 males) and 17 patients with AD (age: 77.6±10.0; 9 males). The two groups were not perfectly age-matched. This might later introduce biases. However, it was shown in a previous study that no major effects stemming from this disparity were found (Henderson et al., 2006). The patient group underwent full cognitive tests, but no neuro-imaging study or neuropsychological scores were available due to disparity among patients' districts. EEG time series were recorded at a sampling frequency of 128 Hz using 19 electrodes disposed according to the Maudsley System, which is similar to the 10-20 international system.

Database B was composed of age-matched subjects, including 5 healthy control subjects (age: 76.6±5.6; 3 males; MMSE: 29.3±0.7) and 5 AD patients (age: 78.8±2.4; 2 males; MMSE: 22.3±3.1). The AD patients were diagnosed according to the NINCDS-ADRDA and DSM IV criteria and underwent general medical, neuromedical, and psychiatric assessments. The cognitive evaluation included a large number of tests such as the MMSE (Mini Mental State Examination), Clinical Dementia Rating Scale (CDRS), and Geriatric Depression Scale (GDS). EEG time series were recorded at a sampling frequency 8 of 128 Hz using 21 electrodes disposed according to the 10-20 international system.

EEGs were band-pass filtered with digital 2nd order Butterworth filter (forward and reverse filtering) between 0.5 and 30 Hz (a sampling rate of 128 Hz means that frequencies above 25 Hz cannot be reliably studied (Barlow, 1993)). All recordings are in rest condition. The two databases were pooled for the analysis, into a combined set of 29 early AD patients and 22 Control subjects.

2.2 Signal Processing

2.2.1 Independent Component Analysis

ICA pre-processing of data was performed using ICAlab ver 3.0, with the IWASOBI algorithm. Time-frequency sparse modeling was performed using Matlab ® 7.0, and the ButIf toolbox (Vialatte et al., 2009c). Three EEG researchers visually inspected EEGs, and each recording's least corrupted continuous 20 sec interval were chosen for the analysis. Each trial was then decomposed using ICA, and artifacts (drifts, eye blinks, sharp waves, abnormal amplitude sources) were removed independently using the procedure detailed in (Vialatte et al., 2009d).

2.2.2 Wavelets Time-frequency Representation

EEG signals were first transformed to a time-frequency representation using complex Morlet wavelets. Wavelets (see (Mallat, 1999; Percival and Walden, 2000) for details), especially complex Morlet wavelets (Kronland-Martinet et al., 1988), have already been widely used for time-frequency analysis of EEG signals (Tallon-Baudry et al., 1996; Düzel et al., 2003; Caplan et al., 2001; Li et al., 2007; Slobounov et al., 2008; Vialatte et al., 2008b; Vialatte et al., 2009a). Complex Morlet wavelets ϑ of Gaussian shape in time (deviation σ) are defined as:

$$\vartheta(t) = A.\exp\left(\frac{-t^2}{2\sigma^2}\right).\exp\left(2i\pi ft\right), \qquad (1)$$

where σ and f are interdependent parameters, linked with the constraint $2\pi ft > 5$. The wavelet family defined by $2\pi ft = 7$, as described in (Tallon-Baudry et al., 1996), is adapted to the investigation of EEG signals. This wavelet has positive and negative values resembling those of an EEG, but also a symmetric Gaussian shape both in the time and frequency domains - *i.e.* this wavelet locates accurately time-frequency oscillations both in the time and frequency domain.

We scale complex Morlet wavelet ϑ to compute time-frequency wavelet representations of the signal $\mathbf{X}$ of length T:

$$C_x(t,s) = \int_T \mathbf{X}(\tau)\vartheta^*\left(\frac{\tau - t}{s}\right)d\tau, \qquad (2)$$

where s, the scaling factor, controls the central frequency f of the mother wavelet. The modulus of this time-scale representation can therefore be used

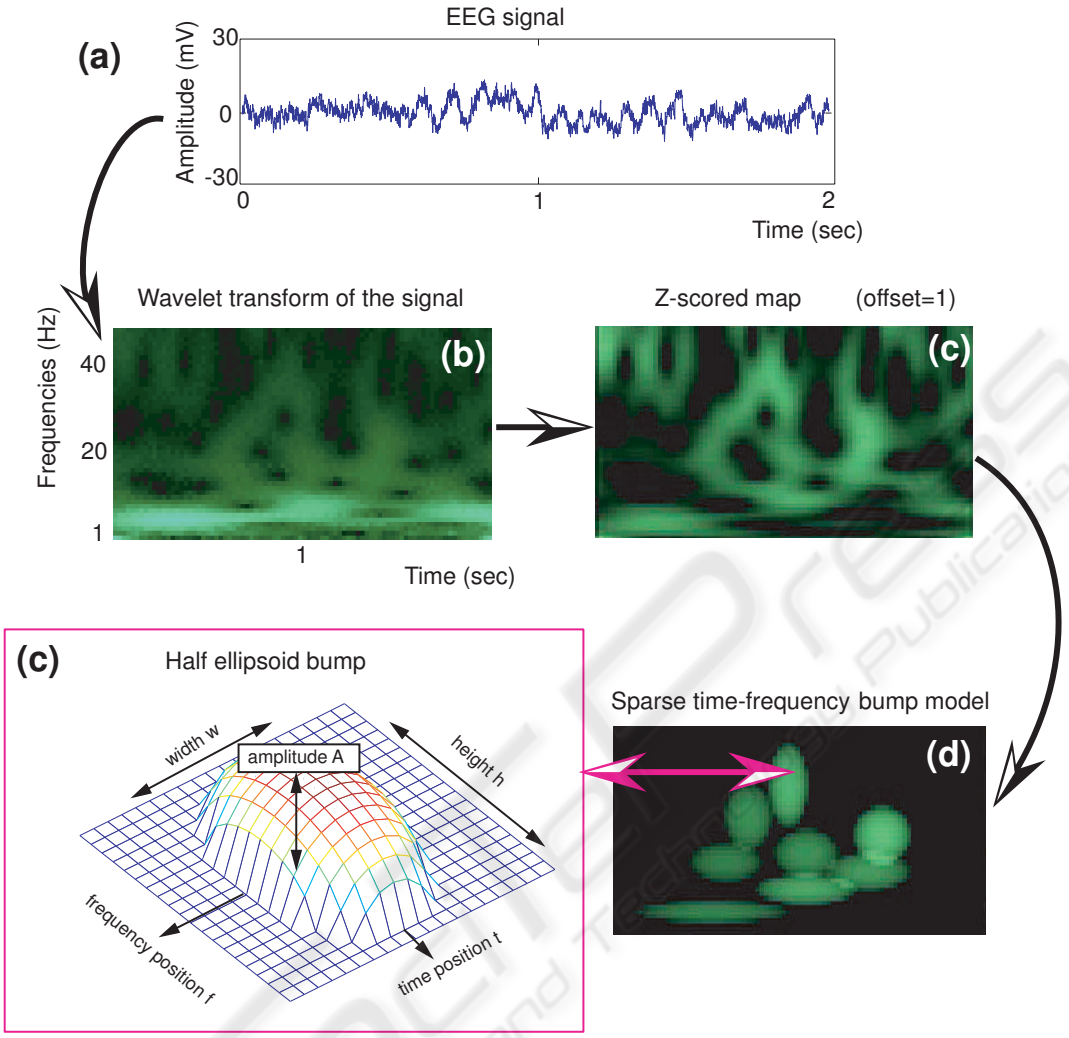

Figure 1: Principle of sparse time-frequency bump modeling.

as a positive time-frequency spectrogram, noted $\mathbf{C_x}$. $\mathbf{C_x}$ is a time-frequency matrix of dimension $T \times F$, where F scales are used to compute appropriate frequency steps (usually linear or logarithmic, in the case of bump modeling we use linear steps).

2.2.3 Bump Modeling

The bump modeling method is covered in detail in (Vialatte et al., 2007; Vialatte et al., 2009c). The principle is illustrated on Figure 1. The wavelet map was computed from 4 to 25 Hz with 0.25 Hz steps, and afterwards normalized using a z-score normalization (see *e.g.* (Vialatte et al., 2008b)). We then modeled the oscillatory patterns present in the normalized time-frequency map:

$$E(A,h,w,f,t,y,x) = \sum_{x=1}^{W}\sum_{y=1}^{H} \|\omega_{y,x}(s,\tau) - \xi\|^2, \quad (3)$$

where the sums are computed over a set of windows, $\xi(A,h,w,f,t,y,x)$ are half-ellipsoid functions, y and x are respectively the time and frequency position of the adaptation window on the time-frequency map (fixed parameters), f and t are respectively the time and frequency position of the bump on the time-frequency map, h and w are respectively the height and width of the bump, A is the amplitude of the bump, and $\|.\|$ is a Frobenius norm. Adaptation is performed using a combination of first and second order gradient descent. The results presented here were obtained with a pruning threshold $F_t = 0.30$, and a z-score offset $\phi = 0$.

3 RESULTS

3.1 Statistical Analysis

We compared the statistics of EEG power before (using the wavelet map before and after z-score) and after bump modeling (using the amplitude A of the bumps in the frequency range), in three frequency ranges: θ (4-8 Hz), α (8-12 Hz), and β (12-25 Hz). These results are computed in relative power (the power in each frequency range is divided by the total power). First, we compared the general average over all electrodes for each patient, and for each of the three frequency ranges, using a Mann-Whitney test[1] (Table 1). The difference of power between the control subjects and the mildAD patients is increased after modeling in the θ and β ranges, but slightly decreased in the α range. The variability of EEG power did not differ between mildAD or controls, wether for wavelets or bumps (Levene test $p >> 0.10$). However, if we compare the distributions before and after bump modeling, the intra-group variability (midlAD *vs.* mildAD, and controls *vs.* controls) is significantly decreased in the α and β ranges (Table 2).

Table 1: Difference between mildAD patients and Control subjects, before and after the wavelet map is modeled with bumps (relative power, all subjects from databases A and B grouped). The p-value, Mann-Whitney z-score statistic, and Bonferroni corrected p-values are displayed. All p-values are highly significant ($p < 0.01$ after correction).

Frequency range (Hz)	Wavelets p-value (Z, corrected p)	Bumps p-value (Z, corrected p)
θ (4-8)	$1.02 \cdot 10^{-5}$ (-4.4, $6.12 \cdot 10^{-5}$)	$7.40 \cdot 10^{-9}$ (-5.8, $4.44 \cdot 10^{-8}$)
α (8-12)	$3.67 \cdot 10^{-5}$ (4.1, $2.20 \cdot 10^{-4}$)	$8.16 \cdot 10^{-4}$ (3.3, $4.90 \cdot 10^{-3}$)
β (12-25)	$3.99 \cdot 10^{-5}$ (4.1, $2.39 \cdot 10^{-4}$)	$5.14 \cdot 10^{-7}$ (5.0, $3.08 \cdot 10^{-6}$)

3.2 Classification

Classification of the whole database was compared, using either the amplitude on the wavelet map, or from the bump modeling. We used a linear classifier (linear discriminant analysis) in a leave-one-out scheme (Stone, 1974). The relative power of all frequency ranges, computed for each patient, was used as an input feature. The learning error decreased from 15.7% for wavelets (illustrated on Figure 2), to 2.9% for bump models (illustrated on Figure 3). The classification error decreased from 25.5% (wavelets) to 11.8% (bumps), this result being mostly due to the improved separation of the θ range (see the Table 3).

[1]Wavelet coefficients are usually not distributed according to a normal distribution, hence a non-parametric test has to be used.

Table 2: Intra-group difference as measured by a Levene test for homoscedasticity. The test measure variations of the standard deviation before and after bump modeling (a positive p-value indicates a decrease or an increase in the intra-group difference). Here, all the significant p-values are indicative of a decrease (mildAD patients became more similar to other mildAD patients after bump modeling, and likewise for control subjects). The p-values are indicated before and after Bonferroni correction. * significant p-value ($p < 0.05$ after correction); ** highly significant p-value ($p < 0.01$ after correction).

Frequency range (Hz)	Controls p-value (corrected p)	MildAD p-value (corrected p)
θ (4-8)	0.0032 (0.019*)	0.0065 (0.039*)
α (8-12)	0.0013 (0.0078**)	$9.36 \cdot 10^{-4}$ (0.0056**)
β (12-25)	0.5343 (1)	0.5784 (1)

Table 3: Classification results (leave-one-out validation), per frequency range.

Frequency range (Hz)	Wavelet % validation error	Bumps % validation error
θ (4-8)	25.49%	11.76%
α (8-12)	27.45%	31.37%
β (12-25)	25.49%	15.69%
global	25.49%	11.76%

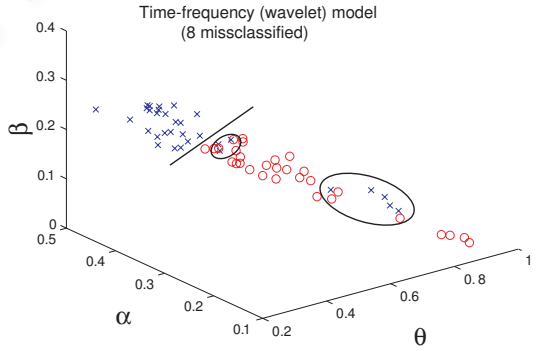

Figure 2: Linear classification using relative power of the wavelet map (both databases A and B). Cross = control subjects, Circle = mildAD patients. The line separates the two classes, circled subjects are misclassified (8 missclassified in total = 15.7%).

A better classification rate should be obtained with optimized parameter combinations (using feature selection) together with a more complex classifier; this is however out of the scope of the present investigation.

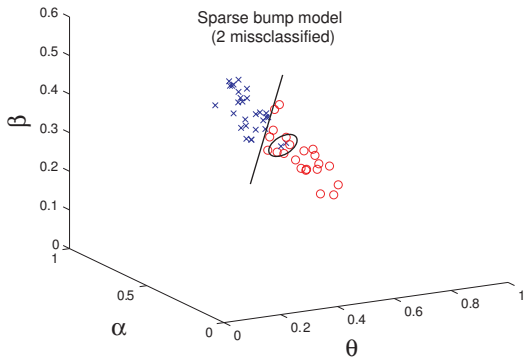

Figure 3: Linear classification using relative power of the sparse bump modeling (both databases A and B). Cross = control subjects, Circle = mildAD patients. The line separates the two classes, circled subjects are misclassified (2 missclassified in total = 2.92%).

4 CONCLUSIONS

We observed that organized oscillatory events contain stronger discriminative signatures of mildAD than averaged spectral EEG statistics. Similarly to our previous results on patients in the early stage of Alzheimer's disease, using another database of patients in MCI (mild cognitive impairment) stage *vs.* Control subjects (Vialatte et al., 2008a), bump modeling improved the separation between mildAD patients and control subjects, specifically in the θ and β ranges. Furthermore, the intra-group variablity was significantly reduced after bump modeling in the θ and α ranges. Finally, this statistical improvement led to a decreased error rate. We were thus able to confirm here our previous observations, using a different database.

Background activity in EEG is mostly attributed to cortical neural events (Barlow, 1993); on the other hand, the oscillatory bursts, generated by locally synchronous neural populations, could be related to inter-area interactions, including sub-cortical areas. Indeed, low-frequency synchrony is probably representative of cortico-subcortical connectivity (Uhlhaas and Singer, 2006). Subcortical damages are induced in the early stage of Alzheimer's disease, and have been correlated with low-frequency power changes (Helkala et al., 1996; Fernández et al., 2003). As a conclusion, using bump modeling allowed us to classify the two groups specifically in the θ and β range. We postulate that the observed strong increase of θ range transient oscillatory activity could be a correlate of sub-cortical damages.

ACKNOWLEDGEMENTS

FBV thanks Prof. J. Jeong for having allowed his visit to KAIST. JSC's work has been supported by the "Programa José Castillejo 2008" from Spanish Government under the grant JC2008-00389, and by the University of Vic under de grant R0904. EEG databases were collected within the Biopattern project, in collaboration with the Plymouth University, UK.

REFERENCES

Başar, E. (1980). *EEG-brain dynamics: Relation between EEG and brain evoked potentials*. Elsevier, Amsterdam.

Barlow, J. (1993). *The Electroencephalogram: Its Patterns and Origins*. MIT Press, Cambridge MA, USA.

Caplan, J., Madsen, J., Raghavachari, S., and Kahana, M. (2001). Distinct patterns of brain oscillations underlie two basic parameters of human maze learning. *J Neurophysiol*, 86(1):368–380.

Düzel, E., Habib, R., Schott, B., Schoenfeld, A., Lobaugh, N., McIntosh, A. R., Scholz, M., and Heinze, H. J. (2003). A multivariate, spatiotemporal analysis of electromagnetic time-frequency data of recognition memory. *Neuroimage*, 18:185–197.

Fernández, A., Arrazola, J., Maestú, F., Amo, C., Gil-Gregorio, P., Wienbruch, C., and Ortiz, T. (2003). Correlations of hippocampal atrophy and focal low-frequency magnetic activity in alzheimer disease: volumetric mr imaging-magnetoencephalographic study. *AJNR Am J Neuroradiol*, 24(3):481–487.

Helkala, E., Hänninen, T., Hallikainen, M., Könönen, M., Laakso, M., Hartikainen, P., Soininen, H., Partanen, J., Partanen, K., Vainio, P., and Riekkinen, P. S. (1996). Slow-wave activity in the spectral analysis of the electroencephalogram and volumes of hippocampus in subgroups of alzheimer's disease patients. *Behav Neurosci*, 110(6):1235–1243.

Henderson, G., Ifeachor, E., Hudson, N., Goh, C., Outram, N., Wimalaratna, S., Del Percio, C., and Vecchio, F. (2006). Development and assessment of methods for detecting dementia using the human electroencephalogram. *IEEE Transaction on Biomedical Engineering*, 53:1557–1568.

Jeong, J. (2004). Eeg dynamics in patients with alzheimers disease. *Clinical Neurophysiology*, 115:1490–1505.

Klimesch, W., Sauseng, P., Hanslmayr, S., Gruber, W., and Freunberger, R. (2007). Event-related phase reorgani-

zation may explain evoked neural dynamics. *Neuroscience and biobehavioral reviews*, 31(7):1003–1016.

Kronland-Martinet, R., Morlet, J., and Grossmann, A. (1988). Analysis of sound patterns through wavelet transforms. *International Journal on Pattern Recognition and Artificial Intelligence*, 1(2):273–301.

Li, X., Yao, X., Fox, J., and Jefferys, J. (2007). Interaction dynamics of neuronal oscillations analysed using wavelet transforms. *Journal of Neuroscience Methods*, 160(1):178–185.

Mallat, S. (1999). *A wavelet tour of signal processing, 2nd edition*. Academic Press, New York.

Moratti, S., Clementz, B., Gao, Y., Ortiz, T., and Keil, A. (2007). Neural mechanisms of evoked oscillations: Stability and interaction with transient events. *Human Brain Mapping*, 28(12):1318–1333.

Nikulin, V., Linkenkaer-Hansen, K., Nolte, G., Lemm, S., Müller, K., Ilmoniemi, R., and Curio, G. (2007). A novel mechanism for evoked responses in the human brain. *European Journal of Neuroscience*, 25(10):3146–3154.

Percival, D. and Walden, A. (2000). *Wavelet Methods for Time Series Analysis*. Cambridge University Press, New York.

Quiroga, R., Sakowitz, O., Başar, E., and Schürmann, M. (2001). Wavelet transform in the analysis of the frequency composition of evoked potentials. *Brain Research Protocols*, 8:16–24.

Slobounov, S., Hallett, M., Cao, C., and Newell, K. (2008). Modulation of cortical activity as a result of voluntary postural sway direction: An eeg study. *Neuroscience Letters*, 442(3):309–313.

Stone, M. (1974). Cross-validatory choice and assessment of statistical predictions (with discussion). *Journal of the Royal Statistical Society B*, 36:111–147.

Tallon-Baudry, C., Bertrand, O., Delpuech, C., and Pernier, J. (1996). Stimulus specificity of phase-locked and non-phase-locked 40 hz visual responses in human. *Journal of Neuroscience*, 16:4240–4249.

Uhlhaas, P. and Singer, W. (2006). Neural synchrony in brain disorders: relevance for cognitive dysfunctions and pathophysiology. *Neuron*, 52:155–168.

Vialatte, F., Bakardjian, H., Prasad, R., and Cichocki, A. (in press 2009a). Eeg paroxysmal gamma waves during bhramari pranayama: A yoga breathing technique. *Consciousness and Cognition*.

Vialatte, F., Dauwels, J., Maurice, M., Yamaguchi, Y., and Cichocki, A. (2009b). On the synchrony of steady state visual evoked potentials and oscillatory burst events. *Cognitive Neurodynamics*, 3(3):251–261.

Vialatte, F., Martin, C., Dubois, R., Haddad, J., Quenet, B., Gervais, R., and G, D. (2007). A machine learning approach to the analysis of time-frequency maps, and its application to neural dynamics. *Neural Networks*, 20:194–209.

Vialatte, F., Maurice, M., and Cichocki, A. (2008a). Why sparse bump models? In *Proceedings of OHBM meeting: June 15-19 2008, Melbourne, Australia - Neuroimage, 41(S1):S159*.

Vialatte, F., Solé-Casals, J., and Cichocki, A. (2008b). Eeg windowed statistical wavelet scoring for evaluation and discrimination of muscular artifacts. *Physiological Measurements*, 29(12):1435–1452.

Vialatte, F., Solé-Casals, J., Dauwels, J., Maurice, M., and Cichocki, A. (2009c). Bump time-frequency toolbox: a toolbox for time-frequency oscillatory bursts extraction in electrophysiological signals. *BMC Neuroscience*, 10(46).

Vialatte, F. B., Solé-Casals, J., Maurice, M., Latchoumane, C., Hudson, N., Wimalaratna, S., Jeong, J., and Andrzej, C. (2009d). Improving the quality of eeg data in patients with alzheimers disease using ica. In *Proceedings of t15th International Conference on Neural Information Processing, ICONIP, Auckland, New Zealand, November 25-28 2008 - LNCS, Part II, 5507:979-986*.